



Comprehensive pathological and quantitative morphometric evaluation of unilateral renal ischaemia reperfusion injury in rat model[#]

C. Divya^{1*}, S. S. Devi ², I.S. Sajitha¹, K.S. Prasanna¹, V.N. Vasudevan³,
 Laiju M. Philip⁴, Varuna P. Panicker⁵, K.R. Naidile¹ and P. Gokul⁶

¹Department of Veterinary Pathology, ³Department of Livestock Products Technology, ⁴Teaching Veterinary Clinical complex, ⁵Department of Veterinary Biochemistry, ⁶Department of Veterinary Surgery and Radiology, College of Veterinary and Animal Sciences, Mannuthy, Thrissur, 680651, ²Bioscience Research and Training Centre, Thonnakkal, Thiruvananthapuram, 695317, Kerala, India., Kerala Veterinary and Animal Sciences University, Pookode, Wayanad, Kerala

Citation: Divya, C., Devi, S.S, Sajitha, I.S, Prasanna, K.S, Vasudevan, V.N., Laiju M.P., Varuna P.P., Naidile, K.R. and Gokul, P. 2025. Comprehensive pathological and quantitative morphometric evaluation of unilateral renal ischaemia reperfusion injury in rat model.

J. Vet. Anim. Sci. **56** (4): 585-592

Received: 04.08.2025

Accepted: 06.10.2025

Published: 31.12.2025

Abstract

Renal ischaemia-reperfusion injury (IRI) is a key precipitating factor in acute kidney injury (AKI) and contributes significantly to the development of chronic kidney disease (CKD). Understanding the temporal dynamics of renal tissue alterations following IRI is critical for determining effective therapeutic strategies. This study aimed to investigate the gross morphological, morphometric and histopathological alterations occurring in rat kidneys at distinct time points following unilateral renal IRI. Twenty-eight adult rats were divided into placebo and IRI groups. IRI was induced by clamping the left renal artery and vein for 60 minutes, while placebo animals underwent sham surgery without vascular occlusion. Animals were euthanised on days 7 and 14 post-surgery. Gross morphology, renal dimensions, organ weight and histopathological changes were evaluated and compared across groups. Placebo animals showed no gross or microscopic renal changes across both time points. In contrast, the IRI group exhibited time-dependent progression of renal injury. At day 7, kidneys showed moderate swelling, congestion and reduced corticomedullary demarcation. Histological findings included tubular degeneration, cast formation and interstitial inflammation—indicative of acute injury. By day 14, kidneys displayed severe gross abnormalities including cortical cysts, abscessations and atrophy. Histopathological examination revealed chronic damage with glomerular atrophy, interstitial fibrosis, endothelial injury and abscess formation. The study delineates the temporal evolution of renal damage following unilateral IRI, distinguishing an early phase (day seven) from a later phase (day 14). These findings provide a structural framework for evaluating interventions in experimental nephropathology.

Keywords: Unilateral renal ischaemia-reperfusion injury, gross morphology, morphometry, histopathology, acute kidney injury, rat model

Ischaemia-reperfusion injury (IRI) is a principal cause of acute kidney injury (AKI) and plays a contributory role in the development of chronic kidney disease (CKD) (Khaleq *et al.*, 2020). It arises when the transient cessation of blood flow to the kidney is followed by restoration of perfusion, leading to oxidative stress, inflammation and cellular injury (Lu, 2013; Malek and Nematbakhsh, 2015; Karimi *et al.*, 2022). Clinically, IRI is encountered in settings such as renal

[#]Part of MVSc thesis submitted by first author to Kerala Veterinary and Animal Sciences University

*Corresponding author: divyac@kvasu.ac.in, Ph. 8289879146

Table 1. Table showing histopathological scoring criteria for renal injury

Tissue type	Histological feature	Score
Tubular damage	No damage	0
	Loss of brush border and mild tubular necrosis in <10% area accompanied by intact basal membrane	1
	Loss of brush border and moderate tubular necrosis in 10 – 25% area accompanied by thickened basal membrane	2
	Loss of brush border and moderate to severe tubular necrosis in 26 – 50% area accompanied by thickened basal membrane, inflammation and cast formation	3
	Loss of brush border and severe tubular necrosis in 50 – 75% of area accompanied by thickened basal membrane, inflammation and cast formation	4
	Loss of brush border and severe tubular necrosis in >75% of area accompanied by thickened basal membrane, inflammation and cast formation	5
Endothelial injury	No damage	0
	Endothelial swelling	1
	Endothelial disruption	2
	Endothelial loss	3
Glomerular damage	No damage	0
	Thickening of Bowman's capsule	1
	Retraction of glomerular tuft	2
	Glomerular fibrosis	3
Interstitial damage	No damage	0
	Inflammation/haemorrhage accompanied by necrosis in 1 – 25 % of the area	1
	Inflammation/haemorrhage accompanied by necrosis in 26 – 50 % of the area	2
	Necrosis in 50 – 75 % of the area	3
	Necrosis in > 75 % of the area	4

transplantation (Salvadori *et al.* 2015), major cardiovascular surgery (Mehta *et al.*, 2007), trauma and sepsis (Makris and Spanou, 2016). Understanding the pattern and progression of tissue damage following IRI is essential for developing effective therapeutic interventions.

Animal models of IRI have been widely employed to study renal pathology and evaluate candidate therapeutics (Baracho *et al.*, 2016). Among these, the rat model is considered particularly useful due to its anatomical and physiological relevance and the feasibility of standardised surgical procedures. Unilateral IRI models offer the advantage of preserving overall renal function while enabling the study of injury-specific responses.

Detailed morphologic and histological characterisation at defined time points is crucial for understanding the structural progression of renal IRI. The current study was undertaken to evaluate gross morphological, morphometric and histopathological alterations in the rat kidney at two time points – days seven and 14 following unilateral IRI, thereby facilitating a comprehensive understanding of time-dependent renal tissue responses. Such models not only guide the timing of therapeutic and regenerative interventions but also serve as platforms to assess the efficacies of biomaterials, growth factors, stem cell-based therapies, imaging biomarkers and nephroprotective agents.

Materials and methods

Twenty-eight adult male Sprague Dawley (SD) rats were randomly assigned to two groups: placebo (sham surgery) group and IRI group. Each group consisted of 14 animals, with subgroups sacrificed on days seven and 14 post-surgery ($n = 7$ per time point per group). The study was approved by the Institutional Animal Ethics Committee (Order No: 25/573/2010-AWD dated 12-06-2024, Proposal No: CVAS/MTY/IAEC/24/73).

Unilateral IRI was induced by clamping the left renal artery and vein for 60 minutes under general anaesthesia. Sham-operated rats underwent laparotomy and kidney exposure without vascular occlusion. After surgery, animals were monitored under identical housing and managerial conditions.

At necropsy, kidneys were examined for gross changes including size, colour, surface texture, consistency, capsular integrity and presence of gross abnormalities. Length and width of kidneys were measured with a measuring scale and weight was recorded using a precision digital weighing balance. Left kidneys were fixed in 10 per cent neutral buffered formalin, processed routinely and stained with haematoxylin and eosin (H&E). A semi-quantitative scoring system was employed to assess renal injury in the tubular, glomerular, endothelial and interstitial compartments (Table 1) adapted from the

criteria described by Khalid *et al.* (2016), Oliveira *et al.* (2019) and Wu *et al.* (2021) in various kidney injury models in rats. Scores from 20 non-overlapping cortical fields per slide at high power magnification (400 times) were averaged for analysis.

Statistical analyses were performed using SPSS. Kidney length and width between the placebo and IRI groups on both days 7 and 14 were analysed using one-way ANOVA followed by Duncan's Multiple Range Test (DMRT). Within-group comparisons across time points were assessed using repeated measures ANOVA with LSD post-hoc testing. Kidney weight differences between groups on each day were analysed using independent t-tests, while within-group comparisons across time points were evaluated using paired t-tests. Histopathological scores were compared between groups on each day using the Mann-Whitney U test and within-group comparisons across days were assessed using the Wilcoxon signed rank test. Data were expressed as mean \pm standard deviation (SD). A p-value < 0.05 was considered statistically significant.

Results and discussion

Gross morphological evaluation

Gross examination revealed clear time-dependent changes in the left kidney following IRI. On day seven post-

injury, kidneys appeared moderately enlarged and swollen with smooth surfaces (Fig. 1a), mild congestion and reduced corticomedullary demarcation indicating acute inflammation. These features are consistent with early, potentially reversible injury, as described in acute phase IRI models (Wu *et al.*, 2017).

By day 14, gross pathology was markedly more severe and heterogenous. In five of seven animals, large cortical cysts filled with purulent material were observed, indicative of abscess formation (Fig. 1b and Fig. 1c). The remaining two animals exhibited atrophic kidneys with a fibrotic and shrunken appearance. In both cases, cortical thinning, disruption of internal architecture and replacement of functional parenchyma by fluid-filled cavities were evident. These changes reflect irreversible, chronic damage and align with previously described outcomes of sustained ischaemic injury (Khan and Khan, 2015; Ichii *et al.*, 2018).

In placebo animals, kidneys retained a normal appearance with smooth capsule, intact surface and clear corticomedullary demarcation at both 7 and 14 days post-surgery (Fig. 1d). No evidence of congestion, cysts or surface irregularities was observed. These findings confirm that surgical intervention without vascular clamping did not elicit any macroscopic renal damage, in line with previous observations of sham-operated controls (Udupa and Prakash, 2018).

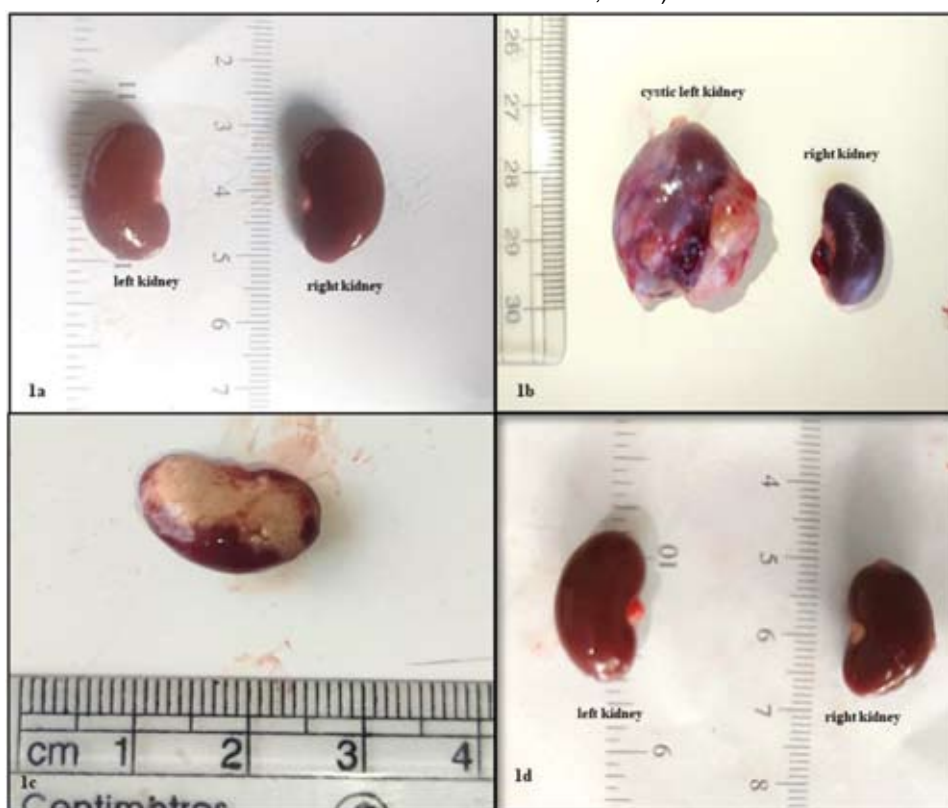


Fig.1. Gross morphological changes observed during IRI. **1a.** Moderately enlarged and swollen left kidney compared to normal right kidney observed 7 days after IRI. **1b.** Left kidney with cystic enlargement and normal right kidney observed 14 days after IRI. **1c.** Left kidney with abscess observed 14 days after IRI. **1d.** Apparently normal right and left kidneys of animals that underwent sham surgery

Table 2. Statistical comparison of length of left kidneys between placebo group and IRI group and also between 7th and 14th day within a group

Group	Day of sacrifice	Day 0	Day of sacrifice	t-value (p-value)
Placebo	7 th day	19.43 ± 0.30	19.71 ^b ± 0.18	1.656 ^{ns} (0.172)
	14 th day	19.43 ± 0.30	19.57 ^b ± 0.30	1.000 ^{ns} (0.356)
IRI group	7 th day	19.43 ± 0.30	22.43 ^{ab} ± 0.30	13.748** (<0.001)
	14 th day	19.43 ± 0.30	23.43 ^a ± 1.95	2.037 ^{ns} (0.088)
F-value (p-value)		0.000 ^{ns} (1.000)	3.756* (0.024)	
** Significant at 0.01 level; * Significant at 0.05 level; ns non-significant Means having different small letter as super script differ significantly within a column				

Table 3. Statistical comparison of width of left kidneys between placebo group and IRI group and also between 7th and 14th day within a group

Group	Day of sacrifice	Day0	Day of sacrifice	t-value (p-value)
Placebo	7 th day	9.86 ± 0.26	10.00 ^b ± 0.22	1.000 ^{ns} (0.356)
	14 th day	10.43 ± 0.20	10.71 ^{ab} ± 0.18	1.549 ^{ns} (0.172)
IRI group	7 th day	9.86 ± 0.26	12.00 ^a ± 0.31	15.000** (<0.001)
	14 th day	9.86 ± 0.26	12.14 ^a ± 1.10	1.804 ^{ns} (0.121)
F-value (p-value)		1.333 ^{ns} (0.287)	3.078* (0.047)	
** Significant at 0.01 level; * Significant at 0.05 level; ns non-significant Means having different small letter as super script differ significantly within a column				

Table 4. Statistical comparison of weight of left kidneys between placebo group and IRI group and also between 7th and 14th day within a group

Time of sacrifice	Placebo group	IRI group	t-value (p-value)
Day 7	0.879 ± 0.013	0.887 ± 0.017	4.483** (0.001)
Day 14	0.947 ± 0.008	1.163 ± 0.097	2.801* (0.029)
t-value (p-value)	1.114 ^{ns} (0.308)	2.258 ^{ns} (0.065)	
** Significant at 0.01 level; * Significant at 0.05 level; ns non-significant			

Gross morphometric evaluation

Morphometric evaluation corroborated these gross findings. In the IRI group, statistically significant enlargement of the kidneys was observed on day 7 post-injury. Compared to 0th day, the length increased from 19.43 ± 0.30 mm to 22.43 ± 0.30 mm and width from 9.86 ± 0.26 mm to 12.00 ± 0.31 mm ($p < 0.001$ for both), as shown in Table 2 and Table 3, respectively. These changes corresponded with the grossly swollen and congested appearance observed in necropsy specimens and are consistent with acute renal inflammation (Wang *et al.*, 2012).

By day 14, the IRI kidneys displayed more heterogeneous changes, reflected in increased variability of morphometric values. The mean length (23.43 ± 1.95 mm) and width (12.14 ± 1.10 mm) showed a continued upward trend, but differences compared to baseline were not statistically significant ($p = 0.088$ and $p = 0.121$,

respectively), likely due to a bimodal distribution. Specifically, five out of seven animals showed cystic enlargement, while two exhibited atrophic shrinkage, inflating the standard deviations and masking significance at the group level. This divergence reflects the dynamic nature of renal repair following IRI, where either compensatory hypertrophy and cyst formation or progressive atrophy and fibrosis may dominate depending on the extent of initial tubular and vascular injury (Koh and Chung, 2024). These findings also emphasise the limitations of relying solely on mean-based statistics in models involving divergent pathological outcomes, reinforcing the importance of qualitative morphological interpretation.

Kidney weight followed a similar pattern. On day seven, the mean weight in the IRI group was 0.887 ± 0.017 g, significantly higher than the placebo group ($p = 0.001$), indicative of inflammatory swelling (Table 4). On day 14, weights ranged widely from 0.78 to 1.41 g, with a mean of 1.163 ± 0.097 g, which was also significantly higher

than the placebo ($p = 0.029$). However, within-group comparison between day 0 and day 14 did not yield statistical significance ($p = 0.065$), attributable to the coexistence of cystic and atrophic changes. The sustained increase in kidney weight up to day 14 suggests that tissue remodelling and ongoing cellular infiltration contributed to mass gain. This interpretation aligns with earlier studies demonstrating that unresolved inflammation and extracellular matrix deposition during the subacute phase can lead to organ enlargement despite progressive tubular necrosis (Ferenbach and Bonventre, 2015). Together, these findings underscore the evolving transition of IRI pathology from acute oedema to chronic remodelling.

In the placebo group, kidney dimensions remained stable over the study period. No significant changes in length or width were noted between day zero and the respective sacrifice days (Days seven and 14), with all p -values > 0.05 (Table 2 and Table 3). Kidney weight also remained within a narrow range (Day 7: 0.879 ± 0.013 g; Day 14: 0.947 ± 0.008 g), with no statistically significant differences over time (Table 4). These results confirmed that the surgical procedure alone, without vascular occlusion, did not elicit gross morphometric alterations, validating the IRI group findings as attributable to the ischaemia-reperfusion insult.

Overall, the morphometric data reflected the dynamic progression of renal injury post-IRI from acute swelling to divergent outcomes of cystic degeneration or atrophy and supported the classification of day seven as a reversible injury phase and day 14 as a chronic, irreversible stage. Importantly, the variability observed at later stages highlighted the importance of complementing quantitative data with morphological observations when interpreting complex injury patterns. In this context, the qualitative assessment of gross pathology remains indispensable, as it captures divergent trajectories that numerical averages may obscure, a point also emphasised in other experimental renal injury models (Bonventre and Yang, 2011).

Histopathological evaluation

Histopathological evaluation of H&E-stained sections revealed a clear progression of renal damage over time in the IRI group, while the placebo group retained largely normal architecture throughout the observation period.

In the IRI group, kidneys examined on day seven post-injury showed characteristic features of acute tubular and interstitial injury including loss of brush border, tubular degeneration (Fig. 2a), cast formation (Fig. 2b), medullary congestion and multifocal interstitial inflammation (Fig. 2c). Mild glomerular atrophy (Fig. 2d) and endothelial alterations were also noted. These lesions were reflected in moderate mean scores for tubular (3.00 ± 0.58) and interstitial (2.57 ± 0.53) damage, while glomerular and

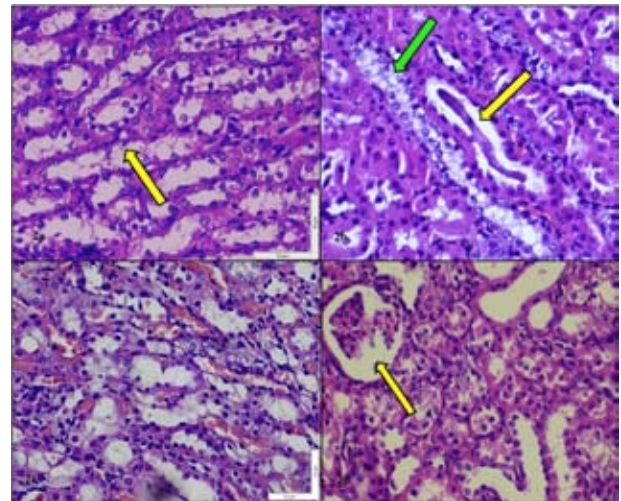


Fig. 2. Histopathological observations at 7 days after IRI. **2a.** Tubular degeneration (yellow arrow) (H&E X 400). **2b.** Intraluminal cast (yellow arrow) and tubular degeneration (green arrow) (H&E X 400). **2c.** Congestion indicative of acute inflammation (H&E X 400). **2d.** Mild glomerular atrophy (H&E X 400)

endothelial compartments showed milder involvement (0.86 ± 0.83 and 1.14 ± 0.83 , respectively). The total score (7.57 ± 1.27) supported the classification of this stage as early phase of kidney injury. These findings are consistent with earlier reports of acute IRI-induced renal changes (Melin, 2002; Furuichi *et al.*, 2009; Shanley *et al.*, 1986; Kim *et al.*, 2011).

By day 14, the IRI kidneys displayed advanced, irreversible injury with widespread tubular degeneration and necrosis (Fig.3a), glomerular and tubular atrophy (Fig.3b), intraluminal cast formation, denudation of basement membrane (Fig.3c), interstitial fibrosis (Fig.

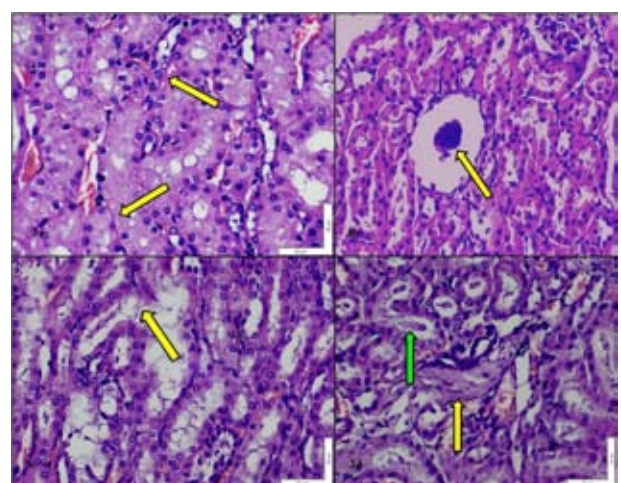


Fig. 3. Histopathological observations at 14 days after IRI. **3a.** Necrosis of tubular epithelial cells (yellow arrow) (H&E X 400). **3b.** Severe glomerular atrophy (yellow arrow) (H&E X 400). **3c.** Tubular degeneration and denudation of basement membrane (yellow arrow) (H&E X 400). **3d.** Interstitial fibrosis (yellow arrow) and tubular cast (green arrow) (H&E X 400).

3d) and dense inflammatory infiltrates in some cases. All compartments were severely affected as reflected by significantly elevated mean scores for tubular (3.86 ± 0.69), glomerular (2.00 ± 0.00), endothelial (2.71 ± 0.49) and interstitial (2.71 ± 0.49) damage. The mean total score rose to 11.29 ± 0.76 . This progression reflects chronic renal pathology, as described earlier in similar IRI models (Wu *et al.*, 2013; Hesketh *et al.*, 2014; Jubb *et al.*, 2016).

Statistical comparison (Table 5) confirmed that histopathologic scores were significantly higher in the IRI group than in the placebo group at both day seven and 14 ($p = 0.001$), with a further significant increase from day seven to 14 within the IRI group ($p = 0.017$), indicating progressive deterioration.

In contrast, the placebo group exhibited minimal changes throughout the study. On both day 7 and day

Table 5. Statistical comparison of histopathologic scores of left kidneys of placebo and IRI groups at day seven and day 14

Time of sacrifice	Placebo group	IRI group	Z-value (p-value)
Day 7	3.571 ± 0.297	7.429 ± 0.481	3.213** (0.001)
Day 14	3.143 ± 0.340	11.286 ± 0.286	3.180** (0.001)
t-value (p-value)	0.750^{ns} (0.453)	2.388^* (0.017)	
** Significant at 0.01 level; * Significant at 0.05 level; ns non-significant			

14, histological findings were largely unremarkable, with preserved renal architecture and only occasional mild tubular or interstitial alterations. Total histopathological scores remained low (3.71 ± 0.49 at day 7 and 3.14 ± 0.90 at day 14), with no significant progression over time ($p = 0.453$). These results confirm that vascular clamping rather than procedural manipulation is the primary determinant of the observed renal injury, thereby validating the model. Similar conclusions were drawn in rodent IRI models by Miao and Han (2024), and Karami *et al.* (2020), who emphasised the role of clamping technique and duration in determining injury severity.

Taken together, the findings confirm that renal injury in IRI progresses over time, beginning with moderate, primarily tubular-interstitial damage and culminating in severe multi-compartmental pathology.

Conclusion

This study provides detailed gross and microscopic evidence of the temporal progression of renal injury following unilateral IRI in rats. A clear distinction between acute and chronic phases of damage was established, with day seven post-injury characterised by reversible inflammatory changes and day 14 reflecting irreversible

degeneration. These findings offer a robust morphological framework for future investigations targeting renal protection and regeneration. The temporal characterisation of injury aids in identifying optimal intervention windows, validating therapeutic strategies and evaluating the efficacy of regenerative biomaterials. Additionally, this model supports applications in nephrotoxicological screening, imaging biomarker validation and pathophysiological studies of renal disease.

Acknowledgement

The authors gratefully acknowledge the Kerala Veterinary and Animal Sciences University (KVASU), Pookode, Wayanad, Kerala, for providing the necessary facilities and institutional support to carry out this research work.

Conflict of interest

The authors declare no conflict of interest.

References

- Baracho, N. C. do V., Kangussu, L. M., Prestes, T. R. R., Silveira, K. D., Pereira, R. M., Rocha, N. P. and Silva, A. C. S. e. 2016. Characterization of an experimental model of progressive renal disease in rats. *Acta Cirurgica Brasileira*. [online]. **31**: 744–752. Available: <https://doi.org/10.1590/S0102-865020160110000007> [15 Jan. 2025].
- Bonventre, J.V. and Yang, L. 2011. Cellular pathophysiology of ischemic acute kidney injury. *J. Clin. Invest.* **121**: 4210–4221.
- Ferenbach, D.A. and Bonventre, J.V. 2015. Mechanisms of maladaptive repair after AKI leading to accelerated kidney ageing and CKD. *Nat Rev Nephrol.* [online]. **11**: 264–76. Available: <https://doi.org/10.1038/nrneph.2015.3> [02 Oct. 2024].
- Furuichi, K., Kaneko, S. and Wada, T. 2009. Chemokine/chemokine receptor-mediated inflammation regulates pathologic changes from acute kidney injury to chronic kidney disease. *Clin. Exp. Nephrol.* [online]. **13**: 9–14. Available: <https://doi.org/10.1007/S10157-008-0119-5> [23 Dec. 2024].
- Hesketh, E.E., Czopek, A., Clay, M., Borthwick, G., Ferenbach, D.A., Kluth, D.C. and Hughes, J. 2014. Renal ischaemia reperfusion injury: a mouse model of injury and regeneration. *J. Vis. Exp.* [online]. **88**: 51816. Available: <https://doi.org/10.3791/51816>. ISSN 1940-087X [05 Nov. 2024].
- Ichii, O., Nakamura, T., Irie, T., Kouguchi, H., Sotozaki, K., Horino, T., Sunden, Y., Elewa, Y.H.A. and Kon, Y. 2018. Close pathological correlations between chronic kidney disease and reproductive organ-

- associated abnormalities in female cotton rats. *Exp. Biol. Med.* [online]. **243**: 418–427. Available: <https://doi.org/10.1177/1535370218758250> [21 Nov. 2024].
- Jubb, K.V.F., Kennedy, P.C. and Palmer, N. 2016. *Pathology of domestic animals*. (6th Ed.). Academic press. In: Elsevier eBooks. <https://doi.org/10.1016/c2012-0-00823-x>
- Karami, M., Owji, S.M. and Moosavi, S.M.S. 2020. Comparison of ischemic and ischemic/reperfused kidney injury via clamping renal artery, vein, or pedicle in anesthetized rats. *Int. Urol. Nephrol.* [online]. **52**: 2415–2428. Available: <https://doi.org/10.1007/S11255-020-02611-X> [17 Aug. 2024].
- Karimi, F., Malek, M. and Nematbakhsh, M. 2022. View of the renin-angiotensin system in acute kidney injury induced by renal ischemia-reperfusion injury. *J. Renin-Angiotensin-Aldosterone Syst.* [online]. 1–10. Available: <https://doi.org/10.1155/2022/9800838>. ISSN 1470-3203 [07 Feb. 2024].
- Khaleq, M.A.A., Hadi, N.R., Hanna, D.B. and Jasim, G.A. 2020. Role of oxidative stress and cytokines in renal ischemia reperfusion injury. *Ann. Trop. Med. Public Health.* [online]. **23**: 23-115. Available: <https://doi.org/10.36295/ASRO.2020.231105> [22 Feb. 2024].
- Khalid, U., Pino-Chavez, G., Nesargikar, P., Jenkins, R.H., Bowen, T., Fraser, D.J. and Chavez, R. 2016. Kidney ischaemia reperfusion injury in the rat: the EGTI scoring system as a valid and reliable tool for histological assessment. *J. Histol. Histopathol.* [online]. **3**: 1. Available: <https://doi.org/10.7243/2055-091x-3-1>. ISSN 2055-091X [30 Aug. 2024].
- Khan, T.M. and Khan, K.N.M. 2015. Acute kidney injury and chronic kidney disease. *Vet. Pathol.* [online]. **52**: 441–444. Available: <https://doi.org/10.1177/0300985814568358> [19 Aug. 2024].
- Kim, J., Kim, J.I., Na, Y.K. and Park, K.M. 2011. Intra-renal slow cell-cycle cells contribute to the restoration of kidney tubules injured by ischemia/reperfusion. *Anat. Cell Biol.* [online]. **44**: 186–193. Available: <https://doi.org/10.5115/ACB.2011.44.3.186> [20 Oct. 2024].
- Koh, E.S. and Chung, S. 2024. Recent update on acute kidney injury-to-chronic kidney disease transition. *Yonsei Med J.* [online]. **65**: 247-256. Available: <https://doi.org/10.3349/ymj.2023.0306> [27 Mar. 2024].
- Lu, C.Y. 2013. The inflammatory response to ischemic acute renal injury. In: Seldin, J. and Giebisch, G. (ed.), *The Kidney: Physiology and Pathophysiology*. (5th Ed.). Elsevier Inc, Philadelphia, USA, 3299p. <https://doi.org/10.1016/B978-0-12-381462-3.00088-4>
- Makris, K. and Spanou, L. 2016. Acute kidney injury: diagnostic approaches and controversies. *Clin. Biochem. Rev.* **37**: 153–175.
- Malek, M. and Nematbakhsh, M. 2015. Renal ischemia/reperfusion injury; from pathophysiology to treatment. *J. Ren. Inj. Prev.* [online]. **4**: 20–27. Available: <https://doi.org/10.12861/JRIP.2015.06>. ISSN 2345-2781 [31 Mar. 2024].
- Mehta, R. L., Kellum, J. A., Shah, S. V., Molitoris, B. A., Ronco, C., Warnock, D. G. and Levin, A. 2007. Acute kidney injury network: Report of an initiative to improve outcomes in acute kidney injury. *Crit. Care.* [online]. **11**: R31. Available: <https://doi.org/10.1186/cc5713>. ISSN 1466-609X [16 Jul. 2024].
- Melin, J. 2002. Renal ischemia/reperfusion injury in diabetes: experimental studies in the rat. Doctoral thesis, Uppsala University, Medicinska vetenskapsområdet, <http://www.divaportal.org/smash/record.jsf?pid=diva2:161515>
- Miao, J. and Han, F. 2024. Bilateral renal ischemia-reperfusion model for acute kidney injury in mice. *J. Vis. Exp.* [online]. **204**: e65838. Available: <https://doi.org/10.3791/65838>. ISSN 1940-087X [15 Jun. 2024].
- Oliveira, A. C. C., Módolo, N. S. P., Domingues, M. A. C. and Schwingel, P. A. 2019. Effects of cyclosporine on ischemia-reperfusion injuries in rat kidneys: an experimental model. *Acta Cir. Bras.* [online]. **34**: e201900806. Available: DOI: <http://dx.doi.org/10.1590/s0102-865020190080000006>. ISSN 1678-2674 [22 Apr. 2024].
- Salvadori, M., Rosso, G. and Bertoni, E. 2015. Update on ischemia-reperfusion injury in kidney transplantation: pathogenesis and treatment. *World J. Transplant.* [online]. **5**: 52–67. Available: <https://doi.org/10.5500/wjt.v5.i2.52>. ISSN 2220-3230 [12 Jan. 2024].
- Shanley, P.F., Rosen, M.D., Brezis, M., Silva, P., Epstein, F.H. and Rosen, S. 1986. Topography of focal proximal tubular necrosis after ischemia with reflow in the rat kidney. *Am. J. Pathol.* **122**: 462–468.
- Udupa, V. and Prakash, V. 2018. Gentamicin induced acute renal damage and its evaluation using urinary biomarkers in rats. *Toxicol. Rep.* [online]. **6**: 91–99. Available: <https://doi.org/10.1016/j.toxrep.2018.11.015>. ISSN 2214-7500 [09 Sep. 2024].

- Wang, H.J., Varner, A., AbouShwareb, T., Atala, A. and Yoo, J.J. 2012. Ischemia/reperfusion-induced renal failure in rats as a model for evaluating cell therapies. *Ren. Fail.* **34**:1324-1332.
- Wu, J., Pan, X., Fu, H., Zheng, Y., Dai, Y., Yin, Y., Chen, Q., Hao, Q., Bao, D. and Hou, D. 2017. Effect of curcumin on glycerol-induced acute kidney injury in rats. *Sci. Rep.* [online]. **7**: 10693. Available: <https://doi.org/10.1038/s41598-017-10693-4>. ISSN 2045-2322 [19 Jul. 2024].
- Wu, Y., Zhang, J., Liu, F., Yang, C., Zhang, Y., Liu, A., Shi, L., Wu, Y., Zhu, T., Nicholson, M.L., Fan, Y. and Yang, B. 2013. Protective effects of HBSP on ischemia reperfusion and cyclosporine A induced renal injury. *Clin. Dev. Immunol.*[online]. **2013**: 758159. Available: doi: 10.1155/2013/758159. ISSN 1740-2530 [14 Apr. 2024].
- Wu, Y., Zwaini, Z., Brunskill, N.J., Zhang, X., Wang, H., Chana, R.S., Stover, C.M. and Yang, B. 2021. Properdin deficiency impairs phagocytosis and enhances injury at kidney repair phase post ischemia-reperfusion. *Front. Immunol.* [online]. **12**: 697760. Available: <https://doi.org/10.3389/FIMMU.2021.697760>. ISSN 1664-3224 [11 Jan. 2024]. ■